Interchain coupling and electron-electron interaction in conjugated polymers

1992 J. Phys.: Condens. Matter 4 5693

(http://iopscience.iop.org/0953-8984/4/26/004)

J. Phys.: Condens. Matter 4 (1992) 5693–5710. Printed in the UK

Interchain coupling and electron–electron interaction in conjugated polymers

Udo Pecher and H Büttner

Physikalisches Institut, Universität Bayreuth, W-8580 Bayreuth, Federal Republic of Germany

Received 21 August 1991, in final form 15 April 1992

Abstract. The influence of the Hubbard interaction on the lattice structure of two half-filled Su–Schrieffer–Heeger chains coupled by constant electron hoppings is examined using a linked cluster expansion of the Gutzwiller variational wave function as well as second-order perturbation theory. Parallel and antiparallel dimerized crystal structures are considered. In the uncorrelated system the metallic undimerized and the insulating parallel dimerized phase compete. However, the state of lowest energy is antiparallel dimerized. In the case of finite Hubbard interaction both the variational and the perturbational approach yield a stabilization of the parallel dimerized configuration. For the parallel dimerized model, the Gutzwiller *ansatz* signals a new ordering of the electrons in the bands: holes are present in the highest occupied single-particle states; the upper valence band is occupied and the lower conduction band is empty even in the 'metallic' phase characterized by crossing bands.

1. Introduction

For quasi-one-dimensional systems it is well known that conductivity depends on the interchain charge transfer sensitively [1, 2]. Recent theoretical work focuses on effects of both *interchain and on-site electron–electron* interaction and *interchain hopping* [3, 4]. It is challenging to consider the influence of the corresponding microscopic parameters on the polymer ground state. As in first-principles calculations [5] we consider two coupled chains. We start from a microscopic level and use the famous SSH model [6] for each chain extended by a constant interchain interaction. This model has been treated before by Baeriswyl and Maki [7], who found that antiparallel ordering of dimerization is favoured for the ground state.

The main objective of this paper is to study the competition of the Hubbard interaction and the interchain hopping. We concentrate on two questions:

(i) Does the Hubbard on-site repulsion change the ground state from antiparallel to parallel ordering?

(ii) Can the interchain hopping suppress the Peierls instability and stabilize the metallic state? (For more information about absence of the Peierls instability see [2, 8, 9].)

The pressure dependence of the energy gap in *trans*-polyacetylene has been contributed to these microscopic interactions recently [10]. Increasing pressure results

0953-8984/92/265693+18$04.50

in a shrinking energy gap [11, 12], which is usually interpreted as an enhanced interchain coupling. *Trans*-$(CH)_x$ exhibits a large negative pressure coefficient and is therefore a promising candidate for achieving a valence–conduction band overlap and thus band conductivity in undoped material. The questions stated above will lead us to this crossing effect automatically. We stress that in this work doping is not considered: the chain orbitals are always half-filled with electrons, and the crossing of bands leads to a new order of the electrons in the bands, but the total electron number is conserved.

The paper is organized as follows: in section 2 we discuss the background of the model relating it to existing experimental and theoretical work. We go on to calculate the exact Peierls energy (section 3), include the Hubbard term (section 4) and using a Gutzwiller variational *ansatz* we derive a simple second-order coefficient called the correlation energy of the expanded ground state energy (section 4). Numerical evaluation of the corresponding formula yields some unexpected results for the dimerization in the case of crossing bands. As a test we apply second-order perturbation theory in section 5, where we find consistency with the variational calculations. Moreover, in the limit of decoupled dimers the system can be solved exactly; this exact ground state energy agrees up to terms of second order in U with our approximate energies (section 5.1). In the last section we discuss the numerical results in detail: in the case of the isomer with parallel dimerization a band overlap is possible. In the absence of Coulomb interaction the isolating dimerized and the metallic undimerized phases compete. Note that the presence of Coulomb interaction favours the dimerized phase. The basis of the Gutzwiller wave function can be a single-particle Slater determinant representing an *excited* state in the uncorrelated case. These excited states can be characterized by full valence and empty conduction bands although the bands cross. In the latter case we call the system 'metallic'. The lattice belonging to these featured states is dimerized.

The comparison between the three isomers shows that the Hubbard interaction determines which structure has the lowest energy. To be more explicit, the Coulomb repulsion reverts the original energy difference between the parallel and antiparallel dimerized structure.

2. Background of the model

There is experimental evidence for a monoclinic structure of the *trans*-$(CH)_x$ unit cell. The precise relation of the two inequivalent chains within the unit cell is still an object of current research [13]. To determine the crystal structure, x-ray and electron diffraction experiments [14–17] have concentrated on measuring the (001) reflection. This peak is for the parallel (antiparallel) dimerized chains allowed (forbidden) and sensitive to bond alternation defects. For example, Kahlert *et al* [16] find an undisturbed $P2_1/a$-crystallized region of 35 Å *only* and state that small parts of their sample are crystallized in the $P2_1/n$ space group. This situation reflects the difficulties in interpreting the experiments and constructing theoretical models. In order to improve the microscopic theory of conjugated polymers [18] it is very appealing to find out which interactions couple the chains significantly.

There exist some tight binding models with various simplifying assumptions for the interchain coupling. Baeriswyl and Maki considered a linear geometry of the chains and couple the directly opposite sites of two chains by constant and alternate hopping

elements, and find antiparallel and parallel dimerized configurations, respectively [7, 19, 20]. In order to simulate the zigzag of the polymer chains, Fesser [21] studied a realistic coupling between one site of a first and three sites of a second chain and found antiparallel ordering. We have seen that the crystallinity of the experimentally available polymer samples is not perfect. Therefore Wolf and Fesser [22] introduced a random contribution in the hopping between two *a priori* parallel dimerized chains. It is well known that high conductivity of polyacetylene can be achieved by doping [23] and doping-induced structural phase transitions were found [24, 25], which may increase the number of chains within the unit cell. Mize and Conwell [26] took these new features into account. In particular, they calculated that the Coulomb potentials of the doping ions shift the bands and lead to partially filled bands. In our model the band overlap is due to the strong interchain hopping only.

The energy gap and the crystal structure of polymers depend on the electron–electron interactions and one has to take care of the correlation effects to explain experiments. Horovitz [27] started with the Fröhlich Hamiltonian, included interchain hopping and considered various electron–electron scattering processes. Primarily, he examined the competition between superconductivity and the Peierls instability. Kivelson and Heim [28] examined 'Hubbard versus Peierls' in a single SSH chain using second-order Goldstone perturbation theory about the Hartree–Fock ground state and in finite rings by studying exact solutions. Jeyadev [4] coupled two SSH chains allowing the full Coulomb potential between all electrons. His calculations applying second-order perturbation theory lead to a parallel dimerized ground state. Baeriswyl and Maki [29] added a Hubbard term to a single SSH chain and used the Gutzwiller wave function to approximate the ground state energy. O'Connor and Watts-Tobin [3] have extended this calculation to a two-chain model for general polyacene [30].

3. Exact Peierls energy

The two coupled chains of conjugated polymers are described by the following Hamiltonian in dimensionless units ($H_0 := H_0/t_0$ and $t_\perp := t_\perp/t_0$ where t_0 is the hopping along an undimerized chain):

$$H_0 = -\sum_{j,n,\sigma} t_{j,n}(c^+_{n+1,j,\sigma}c_{n,j,\sigma} + \text{HC}) - t_\perp(c^+_{n,1,\sigma}c_{n,2,\sigma} + \text{HC}) + N(\Delta/\tilde{\alpha})^2. \quad (1)$$

Here $t_{j,n} = 1 + (-1)^n\Delta$ and $t_{j,n} = 1 + (-1)^{j+n}\Delta$ denote the alternating transfer integrals along the chain j ($j = 1, 2$) with parallel and antiparallel alignment, respectively. The alternating contribution of the transfer term ($\Delta := 2\alpha x/t_0$) is for given electron–phonon coupling proportional to the lattice distortion x (measured in Å). The operators $c^+_{n,j,\sigma}$ ($c_{n,j,\sigma}$) create (annihilate) a π-electron with spin $\sigma = \uparrow, \downarrow$ at site n (n: $-N/2, \ldots N/2 - 1$). Finally, the harmonic force constant is given in dimensionless units by $1/\tilde{\alpha}^2 = \kappa t_0/\alpha^2$ [31].

Primarily, we are interested in the lowest energy of the chains in the presence of period 1 and 2 lattice distortions. Therefore we test the different crystal structures and vary the amplitude of dimerization. The Hamiltonian (1) can be exactly diagonalized: we introduce two ($l = 1, 2$) conduction band ($d^{\text{C}}_{k,l,\sigma}$) and two valence band ($d^{\text{V}}_{k,l,\sigma}$) operators, which are linearly combined and related to the operators in

real space ($c_{n,j,\sigma}$) via Fourier transform. It is obvious that the diagonalizing unitary transformations ((A1), (A3)) as well the diagonalized Hamiltonians ((A6), (A7)) are different for parallel and antiparallel dimerization. The electronic part of the diagonal energy operators runs over all quantum numbers and sums the single-particle energies $E^{C,V}_{k,l}$, which belong to occupied states. For parallel ordering the single-particle energies have the known form [7]

$$E^{C,V}_{k,l} = -(-1)^l t_\perp \pm E_k \tag{2}$$

with the familiar dispersion of the single SSH chain

$$E_k = 2\sqrt{\cos^2 k + (\Delta \sin k)^2}. \tag{3}$$

Band crossing can occur for $t_\perp > 2\Delta_p$; in this case we find $E^C_{\pi/2,2} < E^V_{\pi/2,1}$ at the edges of the Brillouin zone and $E^C_{0,2} > E^V_{0,1}$ at its centre.

The spectrum of antiparallel ordering

$$E^{C,V}_{k,l} = \pm\sqrt{(t_\perp + (-1)^l 2\cos k)^2 + (2\Delta \sin k)^2}. \tag{4}$$

shows no crossing. Obviously, the general ground state of the two coupled chains is given by

$$|g_0\rangle = \prod_{\substack{k \text{ occupied} \\ l,\sigma,A=C,V}} d^{A+}_{k,l,\sigma}|\text{vacuum}\rangle \tag{5}$$

where the different quantum numbers run over the energetically lowest states. Thus, in the case of crossing single-particle energies, the filling of $E^C_{k,2}$ and $E^V_{0,1}$ depends sensitively on the interchain coupling.

In principle the uncorrelated problem is solved. In the next section we will calculate the expectation value of the full Peierls–Hubbard Hamiltonian (an exact diagonalization is not yet possible). We will calculate an upper limit of the ground state energy as a function of certain single-particle expectation values (A8)–(A16). Using these correlation functions we derive for $\varepsilon_0 = \langle g_0|H_0|g_0\rangle$ the exact formula

$$\varepsilon_0 = -4N\left[(1-\Delta)C_{12,\parallel} + (1+\Delta)C_{23,\parallel} + t_\perp C_{11,\perp}\right] + N(\Delta/\tilde{\alpha})^2 \tag{6}$$

which has the same form for parallel and antiparallel dimerization. However, we emphasize that the correlation functions depend sensitively on the ordering of dimerization and especially on the distribution of the electrons in the bands, which we shall call 'band filling'.

4. Variational approach

In this section we apply a variational method to approximate the ground state energy. Firstly the on-site Hubbard term ($U := U/t_0$)

$$H_1 = UD \tag{7}$$

with the projector $D = \sum_j D_j$ and $D_j = \sum_m n_{m,j,\uparrow} n_{m,j,\downarrow}$ is added to the Peierls operator (1). The ground state is constructed by generalizing the Gutzwiller wave function to the two-chain case [32, 33]:

$$|g\rangle = \exp\left(-\frac{1}{2}\sum_j \eta_j D_j\right)|g_0\rangle. \tag{8}$$

The philosophy of this treatment is to find the best correlation paramerters η_j. Because of the model symmetry both variational parameters are equal ($\eta = \eta_1 = \eta_2$). This parameter η describes the degree of the correlations.

The ground state energy can easily be estimated by expanding (8) or using formula (12) in [34]. With $H = H_0 + UD$ and $H_0|g_0\rangle = \varepsilon_0|g_0\rangle$ one immediately obtains

$$\varepsilon = \langle g|H|g\rangle / \langle g|g\rangle = \langle g|H|g\rangle_c \tag{9}$$

$$\varepsilon \simeq \varepsilon_0 + U\langle g_0|D|g_0\rangle - \eta U\langle g_0|D^2|g_0\rangle_c + \tfrac{1}{4}\eta^2\langle g_0|DH_0D|g_0\rangle_c \tag{10}$$

where the subscript c stands for connected diagram contributions (the norm of the Gutzwiller wave function cancels the unlinked graphs). Varying ε with respect to η and abbreviating $|g_0\rangle$ as $\rangle_0$ one finds

$$\eta = 2U\langle D^2\rangle / \langle DH_0D\rangle_{0,c}. \tag{11}$$

Inserting (11) in (10) one obtains the minimized total energy:

$$\varepsilon \simeq \varepsilon_0 + U\langle D\rangle_0 - U^2\langle D^2\rangle^2_{0,c} / \langle DH_0D\rangle_{0,c}. \tag{12}$$

The different expectation values are calculated with the help of (A8)–(A11):

$$\langle D\rangle_0 = \sum_{m,j}\langle n_{m,j,\uparrow}n_{m,j,\downarrow}\rangle_0 = \sum_{m,j}\langle n_{m,j}\rangle_0^2 = 2NC_{11,\|}^2$$

$$\langle D^2\rangle_{0,c} = \sum_{\substack{m,n\\ j,k}}\langle n_{m,k}n_{n,j}\rangle^2_{0,c}. \tag{13}$$

Using Wick's theorem [35], this is equal to

$$\sum_{\substack{m,n\\ j,k}}\left(\langle n_{m,k}\rangle_0\langle n_{n,j}\rangle_0 + \langle c^+_{m,k}c_{n,j}\rangle_0\langle\delta^{j,k}_{m,n} - c^+_{n,j}c_{m,k}\rangle_0\right)^2_c$$

$$= 2N\left[C_{11,\|}^2\left(1 - 2\sum_n\left(C_{1n,\|}^2 + C_{1n,\perp}^2\right)\right) + \sum_n\left(C_{1n,\|}^4 + C_{1n,\perp}^4\right)\right].$$

Restricting to the case of half-filling, one finds after carrying out the different summations that this is equal to

$$2N\sum_n\left(C_{1n,\|}^4 + C_{1n,\perp}^4\right). \tag{14}$$

In order to extract the connected diagrams from $\langle DH_0D\rangle_{0,c}$, the following anticommutator rule is used:

$$K = \{H_0, D\} = \sum_{m,k,\sigma} \left[t_{m,k} \left(c^+_{m+1,k,\sigma} c_{m,k,\sigma} - \mathrm{HC} \right) \left(n_{m+1,k,\bar{\sigma}} - n_{m,k,\bar{\sigma}} \right) \right.$$
$$\left. - (-1)^k t_\perp \left(c^+_{m,1,\sigma} c_{m,2,\sigma} - \mathrm{HC} \right) n_{m,k,\bar{\sigma}} \right] . \tag{15}$$

The denominator of the U^2-coefficient in (12) can be calculated now:

$$\begin{aligned}\langle DH_0D\rangle_{0,c} &= \langle D\,K\rangle_0 \\ &= 2 \sum_{\substack{m,n \\ j,k}} \left[t_{n,k} \left\langle n_{m,j} \left(c^+_{n+1,k} c_{n,k} - \mathrm{HC} \right) \right\rangle_0 \langle n_{m,j} \left(n_{n+1,k} - n_{n,k} \right) \rangle_0 \right. \\ &\quad \left. - t_\perp (-1)^k \langle n_{m,j} \left(c^+_{n,1} c_{n,2} - \mathrm{HC} \right) \rangle_0 \langle n_{m,j} n_{n,k} \rangle_0 \right] \\ &= 4N \left[(1-\Delta) C_{12,\parallel} \left(C_{11,\parallel} - {C_{11,\parallel}}^2 + {C_{12,\parallel}}^2 \right) \right. \\ &\quad + (1+\Delta) C_{23,\parallel} \left(C_{11,\parallel} - {C_{11,\parallel}}^2 + {C_{23,\parallel}}^2 \right) \\ &\quad \left. + t_\perp C_{11,\perp} \left(C_{11,\parallel} - {C_{11,\parallel}}^2 + {C_{11,\perp}}^2 \right) \right] . \end{aligned} \tag{16}$$

For half-filling the total energy including the leading-order correlation energy reads:

$$\varepsilon \simeq \varepsilon_0 + NU/2 - U^2 \varepsilon_{\mathrm{corr}} \tag{17}$$

with

$$\varepsilon_{\mathrm{corr}} = N \left[\sum_n \left(C^4_{1n,\parallel} + C^4_{1n,\perp} \right) \right]^2 \left[(1-\Delta) C_{12,\parallel} \left(\tfrac{1}{4} + {C_{12,\parallel}}^2 \right) \right.$$
$$\left. + (1+\Delta) C_{23,\parallel} \left(\tfrac{1}{4} + {C_{23,\parallel}}^2 \right) + t_\perp C_{11,\perp} \left(\tfrac{1}{4} + {C_{11,\perp}}^2 \right) \right]^{-1} . \tag{18}$$

This formula is valid for both dimerization forms; however, the correlation functions depend on the various dimerizations (A12)–(A16). The energy is numerically evaluated: the sum in the numerator of the correlation energy converges well and is truncated after 100 summands. In the case of vanishing dimerization the value of $\varepsilon_{\mathrm{corr}}$ given in [29, 37] is reproduced.

A characteristic feature of the ground state is the number of pairs per site. Therefore we calculate the number of unprojected pairs per site (the pairs, which survive the on-site repulsion):

$$P = \frac{1}{2N} \langle g | D \mid g \rangle_c \simeq \frac{1}{2N} \left(\langle D \rangle_0 - \eta \langle D^2 \rangle_{0,c} \right) = \frac{1}{4} - \frac{U}{N} \varepsilon_{\mathrm{corr}} . \tag{19}$$

Carmelo *et al* [34] examined the accuracy of the present method for the pure Hubbard model. To be more specific, they compared the above correlation energy as a function of U for half-filling with the exact Bethe solution [36] and found a significant difference for $U > 2t_0$. It is not known, however, whether this deviation signals a similar trend for systems possessing dimerization. In the case of a finite Peierls–Hubbard chain the method of complex-phase averaging [18] allows predictions for the infinite case. Considering a single chain we find a monotonically increasing dimerization for small values of the electron–phonon coupling and a monotonic decreasing one for large $\tilde{\alpha}$ (> 0.7). This is in contrast with [18] where the guess for infinite systems shows a true maximum.

5. Perturbational approach

In addition to the variational approach it is useful to study other methods in order to gain some insight into the coupling mechanism and to test the quality of the variational results. Metzner and Vollhardt [37] showed that second-order perturbation theory [38] yields the exact result [36] for the pure Hubbard model in the weak coupling limit and approximates the exact energy for intermediate coupling strengths ($U < 10t_0$) well. We extend their calculation to the case with dimerization.

5.1. Single chain

In second order the correlation energy is given by

$$\varepsilon_{\mathrm{corr}} := \sum_{\langle e|} \frac{|\langle e|D|g_0\rangle|^2}{E_e - E_0}. \tag{20}$$

In this formulation D (see section 4) produces excited states $|e\rangle$ from the Peierls ground state $|g_0\rangle$. Equation (20) is evaluated in four steps.

(i) First, the unitary transformation, which diagonalizes the unperturbed Hamiltonian, is modified. Therefore new operators with new wave vectors are introduced, which run twice over the Brillouin zone—once over the valence states, the second time over the conduction band (see symbol BZ^2 in (21)).

(ii) Second, D is expressed by these operators and it turns out that the transformed Hamiltonian can be treated more easily, because the scattering between the valence and conducting states is hidden in the amplitude of the perturbation operator.

(iii) Third, it is argued (see [38]) that the normal ordered D acting on a Fermi sea possessing no holes scatters either two particles or none across the Fermi level and that state $\langle e|$ must contain the corresponding excitations.

(iv) Fourth, the four-body expectation value (20) is reduced to the corresponding product of one-particle expectation values using Wick's theorem [35].

The single SSH chain is diagonalized by the transformation (A1) in [29]. We separate this formula in even and odd lattice points in order to get rid of the alternating signs. Introducing the new operators we get

$$c_{2n,\sigma} = \frac{1}{\sqrt{N}} \sum_{l\in \mathrm{BZ}^2} \mathrm{e}^{\mathrm{i}l2n + \mathrm{i}\vartheta_l} a_{l,\sigma} \qquad c_{2n+1,\sigma} = \frac{1}{\sqrt{N}} \sum_{l\in \mathrm{BZ}^2} \mathrm{e}^{\mathrm{i}l(2n+1) - \mathrm{i}\vartheta_l + \mathrm{i}\pi(\lambda_l+1)} a_{l,\sigma} \tag{21}$$

where $a_{l,\sigma}$ annihilates an electron in the band, which is connected to the wave vector via the function

$$\lambda_l = \begin{cases} 1 & \text{if } l \text{ refers to a valence state} \\ 2 & \text{if } l \text{ refers to a conducting state.} \end{cases} \tag{22}$$

Next, we insert transformation (21) into the Hubbard operator of a single chain [29] and obtain

$$D = \frac{1}{N} \sum_{j,k,l,m\in \mathrm{BZ}^2} F_{jklm} a^+_{j,\uparrow} a_{k,\uparrow} a^+_{l,\downarrow} a_{m,\downarrow} \tag{23}$$

with the scattering amplitude

$$F_{jklm} = \tfrac{1}{2}\delta_{l,k-j+m+\nu\pi}\left(e^{i\vartheta_{jklm}} + e^{-i\vartheta_{jklm}+i\pi(\lambda_{jklm}+\nu)}\right) \tag{24}$$

where we have used the abbreviations

$$\vartheta_{jklm} = -\vartheta_j + \vartheta_k - \vartheta_l + \vartheta_m \tag{25}$$

for the phases of the electron states involved and the signs

$$\lambda_{jklm} = -\lambda_j + \lambda_k - \lambda_l + \lambda_m \tag{26}$$

which depend on the combination of scattered valence and conducting states (see (22). Moreover, we take normal ($\nu = 0$) and Umklapp processes ($\nu = \pm 1$) into account. Third, we follow Lindgren and Morrison (section 11.2 in [38]) and calculate the normal ordered D and find that the Hubbard operator acting on a closed electron shell (no holes below the Fermi level) can be reduced to

$$D = -\frac{1}{N}\sum_{k_1,k_2,\bar{k}_1,\bar{k}_2} F_{\bar{k}_1 k_1 \bar{k}_2 k_2} a^{+}_{\bar{k}_1,\uparrow} a^{+}_{\bar{k}_2,\downarrow} a_{k_1,\uparrow} a_{k_2,\downarrow} \tag{27}$$

where the wave vectors k_i run over all occupied and $\bar{k}_i$ over all unoccupied states of $|g_0\rangle$.

Finally, the correlation energy is given by the formula

$$\varepsilon_{\text{corr}} = \frac{1}{N^2}\sum_{k_1,k_2,\bar{k}_1,\bar{k}_2} |F_{\bar{k}_1 k_1 \bar{k}_2 k_2}|^2 \frac{\langle \bar{n}_{\bar{k}_1,\uparrow}\rangle_0 \langle n_{k_1,\uparrow}\rangle_0 \langle \bar{n}_{\bar{k}_2,\downarrow}\rangle_0 \langle n_{k_2,\downarrow}\rangle_0}{E_{\bar{k}_1} + E_{\bar{k}_2} - E_{k_1} - E_{k_2}} \tag{28}$$

with

$$|F_{\bar{k}_1 k_1 \bar{k}_2 k_2}|^2 = \tfrac{1}{2}\delta_{\bar{k}_2,k_1-\bar{k}_1+k_2+\nu\pi}\left[1 + \cos\left(2\vartheta_{\bar{k}_1 k_1 \bar{k}_2 k_2} - \pi(\lambda_{\bar{k}_1 k_1 \bar{k}_2 k_2} + \nu)\right)\right] \tag{29}$$

and with the occupied (unoccupied) single-particle energies E_{k_i} ($E_{\bar{k}_i}$). Here we have used the abbreviation $\rangle_0$ for the Peierls ground state $|g_0\rangle$ and the density operators $n_{k_i,\sigma} = a^{+}_{k_i,\sigma} a_{k_i,\sigma}$ for the electrons and $\bar{n}_{\bar{k}_i,\sigma} = 1 - n_{\bar{k}_i,\sigma}$ for the holes. In the case of half-filling and $N \to \infty$, the formula (28) can be evaluated numerically by standard integration methods.

It is well known that the Peierls energy has two stable minima (see figure 5 in [6]). Surprisingly even the correlation energy is a double-well potential as a function of dimerization (see figure 1). Note the variational and the perturbational results are exactly equal for larger amplitudes of the dimerization. In the limit $\Delta = 1$ the chain decouples into dimers, obviously. Let us expand the exact dimer ground state energy [39] in analogy to (17):

$$\frac{\varepsilon_{\text{Dimer}}}{2} = \frac{U}{4} - t\sqrt{1 + \frac{U^2}{16t^2}} \simeq -t + \frac{U}{4} - U^2\frac{1}{32t}. \tag{30}$$

Setting the dimer hopping element t equal to $1 + \Delta$ we find that its second-order coefficient numerically equals the variational and the perturbational results for $\Delta = 1$.

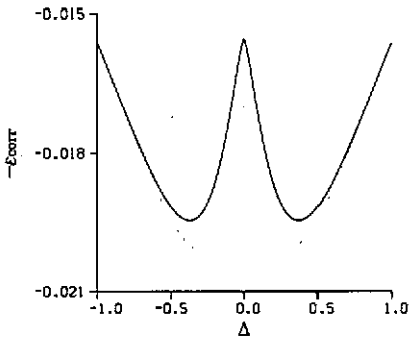

Figure 1. Correlation energy $\varepsilon_{corr}(\Delta)$ per site for $t_\perp = 0$ (in units of t_0). Variational result (18) (solid); perturbational result (28) (dotted).

It is known that the Gutzwiller wave function exactly solves the dimer problem [40]; on the other hand, this limit of the model is unrealistic, as for large displacements the linear dependence of the hopping integral on the lattice coordinates has to be modified and replaced by an exponential dependence (as in the model of Brazovskiĭ *et al* [41]).

We agree with Kivelson and Heim [28] that potentials as in figure 1 enhance the dimerization. However, this potential is only part of the total energy. Obviously the relative position of the minima of ε_0 (ε_0 defined in (6) for $t_\perp = 0$) and of ε_{corr} determines whether the Hubbard-U enhances or reduces the dimerization. We stress that *the electron–phonon coupling* $\tilde{\alpha}$ *shifts the minima of* ε_0 whereas the minima of ε_{corr} are not affected. In contrast to what was found by Kivelson and Heim [28] our correlation energy does not change from a double-well to a parabolic potential for larger U. Therefore we obtain no maximum for Δ as a function of U.

5.2. *Two chains*

The procedure for two chains is equivalent to the case of one. In the appendix we give the modified transformations (A17)–(A24), which are inserted in the Hubbard operator (7). We obtain the square of the scattering amplitudes for parallel ordering:

$$|F_{\bar{k}_1 k_1 \bar{k}_2 k_2}|^2 = \tfrac{1}{16}\delta_{\bar{k}_2,k_1-\bar{k}_1+k_2+\nu\pi}\left(1+\mathrm{e}^{\mathrm{i}\pi\mu_{\bar{k}_1 k_1 \bar{k}_2 k_2}}\right) \times \left[1+\cos\left(2\vartheta_{\bar{k}_1 k_1 \bar{k}_2 k_2}-\pi(\lambda_{\bar{k}_1 k_1 \bar{k}_2 k_2}+\nu)\right)\right] \tag{31}$$

and for antiparallel ordering:

$$|F_{\bar{k}_1 k_1 \bar{k}_2 k_2}|^2 = \tfrac{1}{16}\delta_{\bar{k}_2,k_1-\bar{k}_1+k_2+\nu\pi}\left(1+\mathrm{e}^{\mathrm{i}\pi(\mu_{\bar{k}_1 k_1 \bar{k}_2 k_2}+\nu)}\right) \times \left[1+\cos\left(2\tilde{\vartheta}_{\bar{k}_1 k_1 \bar{k}_2 k_2}-\pi\lambda_{\bar{k}_1 k_1 \bar{k}_2 k_2}\right)\right]. \tag{32}$$

We have introduced the new abbreviations

$$\mu_{jklm} = -\mu_j + \mu_k - \mu_l + \mu_m \tag{33}$$

with

$$\mu_k = \begin{cases} 1 & \text{if } k \text{ refers to } E^{\mathrm{V,C}}_{k,1} \\ 2 & \text{if } k \text{ refers to } E^{\mathrm{V,C}}_{k,2} \end{cases} \tag{34}$$

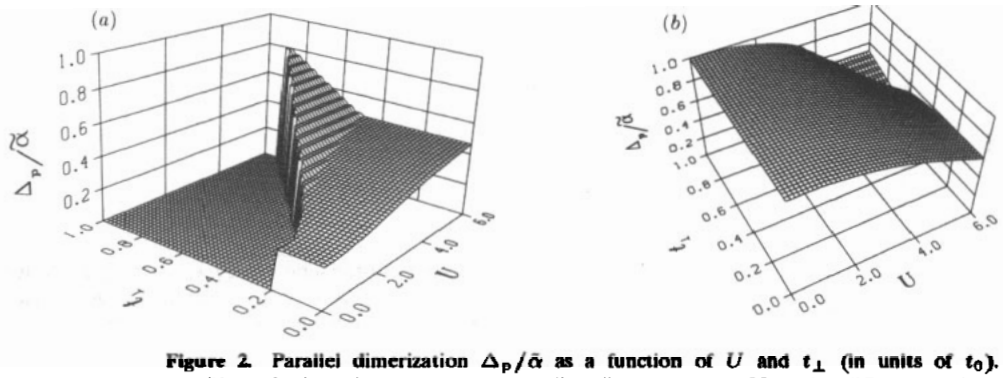

Figure 2. Parallel dimerization $\Delta_p/\tilde{\alpha}$ as a function of U and $t_\perp$ (in units of t_0). (*a*) Dimensionless electron–phonon coupling $\tilde{\alpha}_{SSH} = 0.57$. Note the different regions for the undimerized, metallic state (large $t_\perp$ and U not too large) and the dimerized phase. Perturbation theory leads to the same dependencies. (*b*) Large electron–phonon coupling $\tilde{\alpha} = 1$. Results of perturbation calculation. The corresponding Gutzwiller results decrease similarly as a function of U for small $t_\perp$ and do not depend on $t_\perp$.

and

$$\tilde{\vartheta}_{jklm} = -\vartheta_{j,\mu_j} + \vartheta_{k,\mu_k} - \vartheta_{l,\mu_l} + \vartheta_{m,\mu_m} \tag{35}$$

(ϑ_k and $\vartheta_{k,l}$ are given in the appendix). In contrast to the one-chain model the δ-functions in (31), (32) can additionally scatter the electrons between the bands, which belong to different chains in real space: consider a certain random selection of wave vectors $\bar{k}_1$, k_1, k_2. The wave vector $\bar{k}_2$ lies in the Brillouin zone. Nowhere else are there electron states. Otherwise we have to add a reciprocal-lattice vector. At half-filling, two empty states with the same wave vector are always contained in $|g_0\rangle$. Therefore the resulting $\bar{k}_2$ refers to two states, which belong to different bands. Consequently the Coulomb interaction couples the chains. The correlation energies are calculated using a Monte Carlo integration.

6. Discussion of the results

We summarize the main results first and discuss some details afterwards. For the parallel dimerized model without electronic correlations ($U = 0$), we find a crossing of the upper valence and the lower conduction band, which is related to an insulator–metal transition. If the interchain coupling exceeds a certain threshold value, the dimerization jumps from a finite value to zero, which leads to partially filled bands and to a delocalization of the π-electrons. For the antiparallel dimerized model we find that the amplitude of the dimerization slightly depends on the interchain transfer element. Independently of $t_\perp$, the antiparallel dimerized configuration is energetically favoured in comparison with the undimerized or the parallel dimerized chains.

For finite Coulomb interaction ($U \neq 0$) we find that the energy difference between the undimerized or the parallel dimerized configuration and the antiparallel dimerized structure first increases and then decreases. The number of doubly occupied sites may explain this effect: for finite Hubbard interactions there are more paired electrons in the antiparallel than in the parallel dimerized structure.

Finally, we find that even in the case of band crossing the correlated wave function is favourably constructed by valence states only.

The details are as follows. In the case of parallel dimerization the interchain coupling simply shifts the bands belonging to different chains versus each other. In figure 2(*a*) we show $\Delta_p/\tilde{\alpha}_{SSH}$ as a function of $t_\perp$ and U. For $U = 0$ and increasing $t_\perp$ the amplitude Δ_p does not depend on $t_\perp$. Both valence bands are fully occupied and therefore the correlation function $C_{11,\perp}$ (equation (A13)), which couples the chains, vanishes. Up to a threshold value $t_{\perp,c} \simeq 0.2$ for the electron–phonon coupling $\tilde{\alpha}_{SSH} = 0.57$ the chains behave as an uncoupled system and for all $t_\perp \leqslant t_{\perp,c}$ there exists a finite gap $E_g = 4\Delta_p - 2t_\perp$. For $\Delta_p < t_\perp/2$ the single-particle energies $E^V_{k,1}$ and $E^C_{k,2}$ cross at a certain wave vector k_c. Then the electrons with $k \geqslant |k_c|$ are taken from the V_1 into the C_2 band in order to fill the energetically lowest single-particle states and to avoid holes in the highest occupied single-particle states. For $t_\perp > t_{\perp,c}$ we find $\Delta_p = 0$. In this case one has undimerized metallic chains and the bands could be considered in the original, i.e., extended Brillouin zone: here there are two partially filled cosine bands.

For larger electron–phonon coupling the dimerization and therefore the energy gap increase. For $\tilde{\alpha} = 1$ and $U = 0$ it can be seen from the plot in figure 2(*b*) that the alternating hopping along the chains jumps between 0 and 2, i.e. the electron transfer along the chains is interrupted.

Contrarily, in the case of antiparallel dimerization the interchain coupling acts on the energy bands more complicatedly. In particular, there is no crossing between the higher valence and the lower conduction band. Instead, these bands seem to repel each other in order not to cross. Moreover, the two valence (conduction) bands are not independent functions of $t_\perp$ explicitly they are always degenerate for $k = \pm\pi/2$ and arbitrary $t_\perp$.

In figure 3 we have calculated $\Delta_{ap}/\tilde{\alpha}$ in analogy to figure 2. For $U = 0$ it is seen that strong interchain coupling slightly decreases but cannot destroy the dimerization. The increase of the electron–phonon coupling leads to larger dimerizations, but there is no electronic decoupling along the chains for stronger $\tilde{\alpha}$, because the directly opposite bands differ by 2Δ.

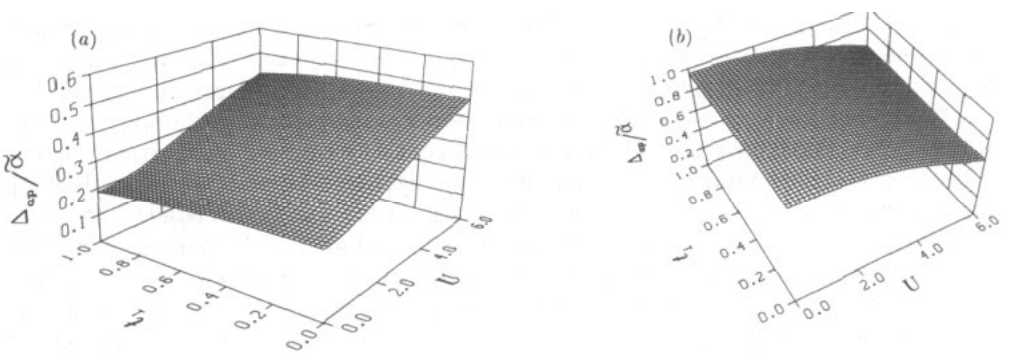

Figure 3. Antiparallel dimerization $\Delta_{ap}/\tilde{\alpha}$. The system depends only weakly on the strength of $t_\perp$. (*a*) For electron–phonon coupling $\tilde{\alpha}_{SSH} = 0.57$ (Gutzwiller results). (*b*) For electron–phonon coupling $\tilde{\alpha} = 1$ (perturbational results). Note the negative slope as a function of U. The Gutzwiller and the perturbation methods give the same dependencies on the parameters for (*a*) and (*b*).

In formula (19) we have shown that the Hubbard interaction breaks up some pairs and therefore influences the ground state and its dimerization. In the case of the

parallel dimerized model figure 2(*a*) shows that the on-site repulsion increases $t_{\perp,c}$. For $t_\perp < t_{\perp,c}$ it is found that the valence (conduction) bands are full (empty) and therefore $C_{11,\perp}$ vanishes, i.e. the total energy (equation (17)) does not depend on $t_\perp$. Nevertheless, there are two different phases, which are distinguished by $E_g > 0$ ($t_\perp$-independent phase) and $E_g = 0$ (U-independent phase). While in the first phase the chains are actually decoupled, in the U-independent phase there is a competition between the lattice energy and the 'band filling' for increasing $t_\perp$. The result is that the V_1 and the C_2 band only touch each other but do not overlap, and that the more favourable 'band filling' compensates the increase of the lattice energy. Obviously, whether one projects pairs from full valence bands or from a mixture of valence and conducting states makes a difference.

The variational and the perturbational approach both lead to the same amplitude of the dimerization, but there are significant energy differences, which have to do with the competition between 'band filling' and lattice.

In figure 2(*b*) we show perturbational results for strong electron–phonon coupling. For small U the decrease of the dimerization does not depend on $t_\perp$. In contrast to the variational results the dimerization for larger U depends on $t_\perp$. For parameters U, $t_\perp$ both large, the 'band filling' effect stabilizes the dimerization and leads again to an U-independent phase.

Within the antiparallel dimerized model there are no exceptional influences of U on the dimerization. Both approaches agree for the different electron–phonon couplings: in figure 3(*a*) we show that for $\tilde{\alpha}_{SSH}$ the dimerization is increased by U and in figure 3(*b*) that for strong electron–phonon coupling the dimerization is decreased by the on-site repulsion.

Next, we want to demonstrate that an increase of the Hubbard interaction leads to a stabilization of the parallel dimerized structure. We calculate the energy difference between the lattice structures given in the figures 2(*a*) and 3(*a*). The results are shown in figure 4(a): for increasing Hubbard U the energy difference first increases then decreases; finally the parallel dimerized structure becomes stable (negative value of $\delta\varepsilon_\Delta$ in figure 4(*a*)). Figure 4(*b*) suggests a possible explanation: for a small on-site repulsion the number of paired electrons on the undimerized chains is greater than in the stable antiparallel dimerized phase. Stronger electron–electron interactions lead to parallel dimerization with fewer pairs than the antiparallel dimerized phase.

These dependences on U are conserved for stronger electron–phonon coupling. It seems possible that a change of the microscopic parameters by external impacts leads to new conformations as for example in the hydrogen-bonded polymer HBr [42], which goes at high pressure from the asymmetric to the symmetric bonded phase.

Based on these results we propose a new 'band filling' for the parallel dimerized model. As we have seen in figure 2(*a*) there has been a competition between lattice energy and 'band filling', which has led to the U-independent phase. Originally, we have operated with the Gutzwiller projector on the true $U = 0$ ground state, but we have found no dimerized 'metallic' ground state. Now we operate on a $U = 0$ excited state: we select an alternative trial wave function, where the valence (conduction) bands are always fully occupied (empty) even in the case of band crossing ($\Delta_p < t_\perp/2$). In other words, to form the $U > 0$ variational state, the Gutzwiller projector $\hat{D}$ acts on an excited eigenstate of H_0, i.e. there are holes in the energetically highest occupied single-particle states. This new feature leads to divergences in the perturbation theory (one has to use the formalism of *open shell* systems [38]). Therefore, we have used the variational approach to calculate the dimerization shown

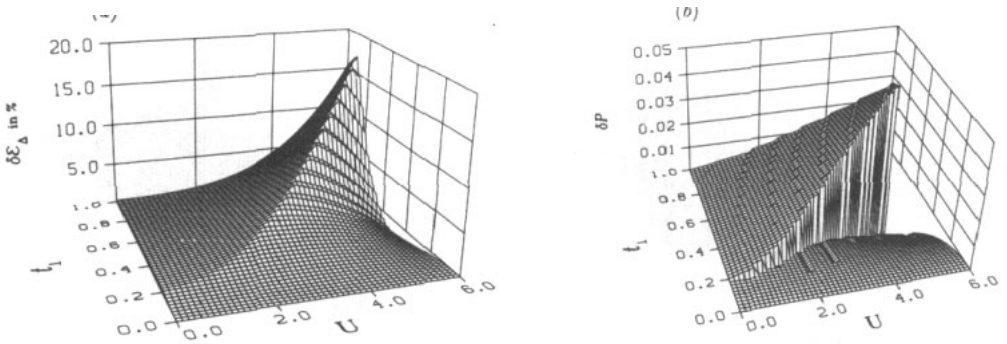

Figure 4. (*a*) Energy difference between the isomer results of figure 2(*a*) and 3(*a*): $\delta\varepsilon_\Delta = 100\,(\varepsilon_{\Delta ap} - \varepsilon_{\Delta p})/\varepsilon_{\Delta ap}$ for $\tilde{\alpha}_{SSH} = 0.57$. Calculation with Gutzwiller correlation energy (18). For finite on-site repulsion $\delta\varepsilon_\Delta$ increases and then decreases. Perturbation theory yields a faster energy stabilization ($\delta\varepsilon_\Delta < 0$ for $U \geqslant 4$) of the parallel dimerized structure than the Gutzwiller expansion. (*b*) The number of the expected pairs $2N\delta P$ on the undimerized or parallel dimerized chains *minus* the pairs on the antiparallel dimerized chains ($\delta P = P_p - P_{ap}$, P from (19)). $U > 0$: in real space the undimerized (metallic) crystal contains the most pairs and the antiparallel dimerized configuration more than the parallel dimerized phase.

in figure 5. The unusual U-independent phase has disappeared and the bands cross. This dimerized 'metallic' state costs slightly more electronic energy, but much less lattice energy. Moreover, the precise comparison between figure 2(*a*) and 5 shows that the new order of the electrons in the bands enhances t_c. Let us list the advantages of the dimerized phase.

(i) The dimerization costs lattice energy and the creation of holes leads to an energy increase for the single particles, which have to leave the conduction band $E^C_{k,2}$.

(ii) The gain of energy is caused by the new dispersions ($E^{C,V}_{k,l}$ depend on Δ) and, what is most important, by the larger correlation energy.

(iii) Finally, figure 6 gives energy-based evidence that the Peierls–Hubbard system prefers valence states as compounds of the correlated wave function.

Applying the model calculations to polyacetylene we choose the standard parameters $\alpha = 4.1$ eV Å^{-1}, $\kappa = 21$ eV Å^{-2}, $t_0 = 2.5$ eV, which lead to $\tilde{\alpha} = \alpha/\sqrt{\kappa t_0} \approx 0.57$. Assuming a realistic interchain hopping parameter less than $0.2\,t_0$ we see from figure 4 that the energy difference between parallel and antiparallel ordering is very small and tends to favour the parallel ordering for larger Hubbard U. Ultimately it seems plausible that $(CH)_x$ is always near the transition between the two phases, which would be consistent with the experiments of Kahlert *et al* [16]. Because of the weak interchain coupling, we do not expect correlation-induced holes in the highest occupied single-particle states.

Note, however, that the theory presented is not limited to polyacetylene. It makes sense to conceive this material as embedded in a theory for general graphite and for the broader class of synthetic metals [18]. Indeed, the newly reported electronic properties of graphitic microtubules depend sensitively on the tubule structure. Using a tight binding method Hamada *et al* [43] find band structures with and without crossing as a function of the various atomic configurations. $M(dmit)_2$ salts [44, 45] also seem to show the strong features of the model with parallel bonds discussed

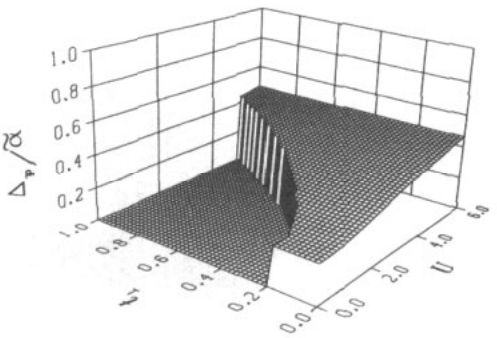

Figure 5. Parallel dimerization. $\Delta_p/\bar{\alpha}_{SSH}$ for the Gutzwiller method. If $E_g = 4\Delta_p - 2t_\perp < 0$ the *dimerized* phase is calculated with an *excited* eigenstate of H_0: in contrast to the Peierls 'band filling' in figure 2(*a*) the valence bands are full and the conduction bands empty. In spite of there being holes in the highest occupied single-particle energy this *new* 'band filling' is energetically preferred.

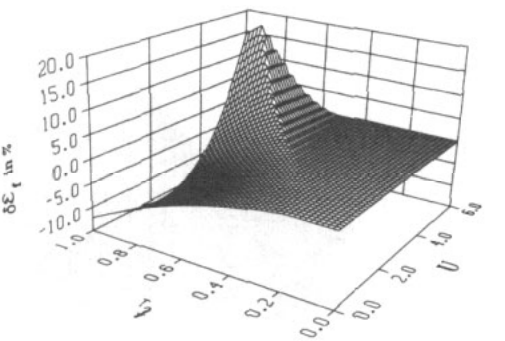

Figure 6. Energy difference for Gutzwiller results based on the *excited* eigenstate of H_0 with full valence (empty conduction) bands ($\varepsilon_{new} < 0$) and based on the ground state of H_0 with Peierls 'band filling' ($\varepsilon_{Peierls} < 0$): $\delta\varepsilon_f = 100\,(\varepsilon_{new} - \varepsilon_{Peierls})/\varepsilon_{new}$ for $\bar{\alpha}_{SSH} = 0.57$ (ε_{new} is stable if $\delta\varepsilon_f > 0$).

above. One only has to replace interchain by interstack interactions: 'The strength of the interstack interactions depends subtly on the interaction geometry, and can be quite strong' [44].

Generally, we agree with Horovitz [27] that pressure increases the interchain coupling, and that above some critical pressure the lattice instability in substances, which cannot arrange the bonds antiparallel, is suppressed. Taking the new correlation effect into account we find that the undimerized phase is always metallic, whereas the dimerized one is insulating only if the bands do not cross.

7. Conclusion

In short, we state the main results of this paper. An increase of the electron–electron on-site repulsion may lead to a transition from an antiparallel dimerized ground state to a parallel one. For finite Hubbard interaction the number of paired electrons in real space depends on the lattice structure under consideration: it is smallest for parallel dimerized chains and largest for undimerized ones. Applying our model calculations to polyacetylene we find that the energy of both the parallel and antiparallel dimerized structures does not differ significantly. The assumption of parallel dimerized bonds enables us to explain that an increase of the interchain hopping may lead to an absence of the lattice instability.

In summary, the variational and perturbational model calculations yield consistent results. It is important to stress that the Gutzwiller variational wave function allows to make different choices for the underlying one-particle wave function. For finite Hubbard interaction and finite dimerization we have found that the Gutzwiller projector operates on fully occupied valence bands even if they cross.

Generally, it is interesting to apply the method to substances as graphitic microtubules [43] and to get more insight in the many-body problem, e.g. to include off-diagonal electron–electron interactions [18].

Acknowledgments

We would like to thank S Weber-Milbrodt for critically reading the manuscript. This work has been supported by the Deutsche Forschungsgemeinschaft through SFB 213 (TOPOMAC, Bayreuth).

Appendix

The pure Peierls Hamiltonian (1) for *parallel* bonds is diagonalized by

$$c_{n,j,\sigma} = \frac{1}{\sqrt{2N}} \sum_k e^{i[kn+(-1)^n \vartheta_k]} \left[(-1)^j (d^V_{k,1,\sigma} + (-1)^n d^C_{k,1,\sigma}) + d^V_{k,2,\sigma} + (-1)^n d^C_{k,2,\sigma}\right] \tag{A1}$$

with the phase

$$\vartheta_k = \tfrac{1}{2} \arctan (\Delta_p \tan k) \tag{A2}$$

and for *antiparallel* bonds by

$$c_{n,j,\sigma} = \frac{1}{\sqrt{2N}} \sum_k e^{ikn} \left[(-1)^j e^{i(-1)^{j+n} \vartheta_{k,1}} (d^C_{k,1,\sigma} + (-1)^{j+n} d^V_{k,1,\sigma}) + e^{i(-1)^{j+n} \vartheta_{k,2}} (d^V_{k,2,\sigma} + (-1)^{j+n} d^C_{k,2,\sigma})\right] \tag{A3}$$

with the phase

$$\vartheta_{k,l} = \tfrac{1}{2} \left[2\Theta \left((-1)^l \Delta_{ap} \sin k\right) - 1\right] \arccos \left(\frac{t_\perp + (-1)^l 2 \cos k}{E_{k,l}} \right) \tag{A4}$$

and the step function

$$\Theta(x) = \begin{cases} 0 & \text{if } x < 0 \\ 1 & \text{if } x \geqslant 0. \end{cases} \tag{A5}$$

The diagonalized energy operators for *parallel* and *antiparallel* bonds are respectively:

$$H_{0,p} = -\sum_{k,l,\sigma} \left[E_k (n^V_{k,l,\sigma} - n^C_{k,l,\sigma}) + (-1)^l t_\perp (n^V_{k,l,\sigma} + n^C_{k,l,\sigma})\right] + \varepsilon_{\text{lattice}} \tag{A6}$$

$$H_{0,ap} = -\sum_{k,l,\sigma} E_{k,l} (n^V_{k,l,\sigma} - n^C_{k,l,\sigma}) + \varepsilon_{\text{lattice}}. \tag{A7}$$

The operators $n^{C,V}_{k,l,\sigma}$ test the number of fermions in the respective states.

Some expectation values appearing in $\langle g_0|H_0|g_0\rangle$ are equal and it is suitable to define some (spin independent) correlation functions. In the case of *parallel* dimerized chains:

$$C_{mn,\parallel} = \langle g_0|c^+_{m,1} c_{n,1}|g_0\rangle = \langle g_0|c^+_{m,2} c_{n,2}|g_0\rangle = \langle g_0|c^+_{n,1} c_{m,1}|g_0\rangle \tag{A8}$$

$$C_{mn,\perp} = \langle g_0|c^+_{m,1} c_{n,2}|g_0\rangle = \langle g_0|c^+_{m,2} c_{n,1}|g_0\rangle = \langle g_0|c^+_{n,1} c_{m,2}|g_0\rangle. \tag{A9}$$

In the case of *antiparallel* dimerized chains:

$$C_{mn,\parallel} = \langle g_0|c^+_{m,2}c_{n,2}|g_0\rangle = \langle g_0|c^+_{m+1,1}c_{n+1,1}|g_0\rangle = \langle g_0|c^+_{n,2}c_{m,2}|g_0\rangle \tag{A10}$$

$$C_{mn,\perp} = \langle g_0|c^+_{m,1}c_{n,2}|g_0\rangle = \langle g_0|c^+_{m+1,2}c_{n+1,1}|g_0\rangle = \langle g_0|c^+_{n,2}c_{m,1}|g_0\rangle. \tag{A11}$$

We insert the operator transformations (A1) and (A3) in the formulas above and obtain for *parallel* ordering

$$C_{mn,\parallel} = \frac{1}{2N}\sum_k \phi_{k,mn}\langle g_0|n^{\mathrm{V}}_{k,1} + n^{\mathrm{V}}_{k,2} + (-1)^{m+n}(n^{\mathrm{C}}_{k,1} + n^{\mathrm{C}}_{k,2})|g_0\rangle \tag{A12}$$

$$C_{mn,\perp} = \frac{1}{2N}\sum_k \phi_{k,mn}\langle g_0|n^{\mathrm{V}}_{k,2} - n^{\mathrm{V}}_{k,1} + (-1)^{m+n}(n^{\mathrm{C}}_{k,2} - n^{\mathrm{C}}_{k,1})|g_0\rangle \tag{A13}$$

with the amplitude

$$\phi_{k,mn} = \cos\left(k(n-m) + [(-1)^n - (-1)^m]\,\vartheta_k\right) \tag{A14}$$

and for *antiparallel* ordering

$$\begin{aligned} C_{mn,\parallel} = \frac{1}{2N}\sum_k \{&\cos\left(k(n-m) + [(-1)^m - (-1)^n]\,\vartheta_{k,1}\right) \\ &\times \langle g_0|n^{\mathrm{C}}_{k,1} + (-1)^{m+n}n^{\mathrm{V}}_{k,1}|g_0\rangle \\ &+ \cos\left(k(n-m) + [(-1)^m - (-1)^n]\,\vartheta_{k,2}\right) \\ &\times \langle g_0|n^{\mathrm{V}}_{k,2} + (-1)^{m+n}n^{\mathrm{C}}_{k,2}|g_0\rangle\} \end{aligned} \tag{A15}$$

$$\begin{aligned} C_{mn,\perp} = \frac{1}{2N}\sum_k \{&-\cos\left(k(n-m) + [(-1)^m + (-1)^n]\,\vartheta_{k,1}\right) \\ &\times \langle g_0|n^{\mathrm{C}}_{k,1} - (-1)^{m+n}n^{\mathrm{V}}_{k,1}|g_0\rangle \\ &+ \cos\left(k(n-m) + [(-1)^m + (-1)^n]\,\vartheta_{k,2}\right) \\ &\times \langle g_0|n^{\mathrm{V}}_{k,2} - (-1)^{m+n}n^{\mathrm{C}}_{k,2}|g_0\rangle\}\,. \end{aligned} \tag{A16}$$

In the case considered infinite chains ($N \to \infty$) and periodic boundary conditions—the correlation functions can be easily evaluated by numerical integration over the Brillouin zone (see [6, 29]).

The unitary transformations (A1), (A3), which diagonalize the two chain models, are redefined to simplify the procedure of second order perturbation theory.

In the case of *parallel* dimerized chains:

$$c_{2n,1,\sigma} = \frac{1}{\sqrt{2N}}\sum_{l\in \mathrm{BZ}^*} \mathrm{e}^{\mathrm{i}l2n + \mathrm{i}\vartheta_l + \mathrm{i}\pi\mu_l} a_{l,\sigma} \tag{A17}$$

$$c_{2n+1,1,\sigma} = \frac{1}{\sqrt{2N}}\sum_{l\in \mathrm{BZ}^*} \mathrm{e}^{\mathrm{i}l(2n+1) - \mathrm{i}\vartheta_l + \mathrm{i}\pi(\lambda_l + \mu_l + 1)} a_{l,\sigma} \tag{A18}$$

$$c_{2n,2,\sigma} = \frac{1}{\sqrt{2N}}\sum_{l\in \mathrm{BZ}^*} \mathrm{e}^{\mathrm{i}l2n + \mathrm{i}\vartheta_l} a_{l,\sigma} \tag{A19}$$

$$c_{2n+1,2,\sigma} = \frac{1}{\sqrt{2N}}\sum_{l\in \mathrm{BZ}^*} \mathrm{e}^{\mathrm{i}l(2n+1) - \mathrm{i}\vartheta_l + \mathrm{i}\pi(\lambda_l + 1)} a_{l,\sigma} \tag{A20}$$

with λ_l defined in (22) and μ_l in 34).

In the case of *antiparallel* dimerized chains:

$$c_{2n,1,\sigma} = \frac{1}{\sqrt{2N}} \sum_{l\in \mathrm{BZ}^4} \mathrm{e}^{\mathrm{i}l2n - \mathrm{i}\vartheta_{l,\mu_l} + \mathrm{i}\pi(\lambda_l+1)} a_{l,\sigma} \tag{A21}$$

$$c_{2n+1,1,\sigma} = \frac{1}{\sqrt{2N}} \sum_{l\in \mathrm{BZ}^4} \mathrm{e}^{\mathrm{i}l(2n+1) + \mathrm{i}\vartheta_{l,\mu_l} + \mathrm{i}\pi\mu_l} a_{l,\sigma} \tag{A22}$$

$$c_{2n,2,\sigma} = \frac{1}{\sqrt{2N}} \sum_{l\in \mathrm{BZ}^4} \mathrm{e}^{\mathrm{i}l2n + \mathrm{i}\vartheta_{l,\mu_l}} a_{l,\sigma} \tag{A23}$$

$$c_{2n+1,2,\sigma} = \frac{1}{\sqrt{2N}} \sum_{l\in \mathrm{BZ}^4} \mathrm{e}^{\mathrm{i}l(2n+1) - \mathrm{i}\vartheta_{l,\mu_l} + \mathrm{i}\pi(\lambda_l+\mu_l+1)} a_{l,\sigma}. \tag{A24}$$

References

[1] Firsov Yu A 1985 *Localization and Metal–Insulator Transition* ed H Fritzsche and D Adler (New York: Plenum)
[2] Wang Z H, Li C, Scherr E M, MacDiarmid A G and Epstein A J 1991 *Phys. Rev. Lett.* **66** 1745
[3] O'Connor M P and Watts-Tobin R J 1988 *J. Phys. C: Solid State Phys.* **21** 825
[4] Jeyadev S 1983 *Phys. Rev.* B **28** 3447
[5] Springborg M 1989 *Phys. Rev.* B **40** 5774
[6] Su W P, Schrieffer J R and Heeger A J 1980 *Phys. Rev.* B **22** 2099
[7] Baeriswyl D and Maki K 1983 *Phys. Rev.* B **28** 2068
[8] Kivelson S and Heeger A J 1988 *Synth. Met.* **22** 371
[9] Paasch G, Lehmann G and Wuckel L 1990 *Synth. Met.* **37** 23
[10] Piccitto G, Pucci R and Grout P J 1991 *Phys. Rev.* B **43** 4224
[11] Moses D, Feldblum A, Ehrenfreund E, Heeger A J, Chung T-C and MacDiarmid A G 1982 *Phys. Rev.* B **26** 3361
[12] Brillante A, Hanfland M, Syassen K and Hocker J 1986 *Physica* B **139/140** 533
[13] Zemach R, Ashkenazi J and Ehrenfreund E 1989 *Phys. Rev.* B **39** 1891
[14] Fincher C R Jr, Chen C-E, Heeger A J, MacDiarmid A G and Hastings J B 1982 *Phys. Rev. Lett.* **48** 100
[15] Moon Y B, Winokur M, Heeger A J, Barker J and Bott D C 1987 *Macromolecules* **20** 2457
[16] Kahlert H, Leitner O and Leising G 1987 *Synth. Met.* **17** 467
[17] Chien J C W, Karasz F E and Shimamura K 1982 *Macromol. Chem.* **3** 655
[18] Campbell D K 1990 *Mol. Cryst. Liq. Cryst.* **189** 65
[19] Baeriswyl D and Maki K 1988 *Phys. Rev.* B **38** 8135
[20] Baeriswyl D and Maki K 1989 *Synth. Met.* **28** D507
[21] Fesser K 1989 *Phys. Rev.* B **40** 1962
[22] Wolf M and Fesser K 1991 *J. Phys. C: Solid State Phys.* **3** 5489
[23] Javadi H H S, Chakraborty A, Li C, Theophilou N, Swanson D B, MacDiarmid A G and Epstein A J 1991 *Phys. Rev.* B **43** 2183
[24] Choi H-Y and Mele E J 1989 *Phys. Rev.* B **40** 3439
[25] Cohen R J and Glick A J 1990 *Phys. Rev.* B **42** 7659
[26] Mizes H A and Conwell E M 1991 *Phys. Rev.* B **43** 9053
[27] Horovitz B 1977 *Phys. Rev.* B **16** 3943
[28] Kivelson S and Heim D E 1982 *Phys. Rev.* B **26** 4278
[29] Baeriswyl D and Maki K 1985 *Phys. Rev.* B **31** 6633
[30] Tanaka K, Ohzeki K, Nankai S, Yamabe T and Shirakawa H 1983 *J. Phys. Chem. Solids* **44** 1069
[31] Waas V, Büttner H and Voit J 1990 *Phys. Rev.* B **41** 9366
[32] Coppersmith S N 1990 *Phys. Rev.* B **41** 8711

[33] Gros C 1989 *Ann. Phys., NY* **189** 53
[34] Carmelo J, Dzierzawa M, Zotos X and Baeriswyl D 1991 *Phys. Rev.* B **43** 598
[35] Mahan G D 1981 *Many Particle Physics* (New York: Plenum)
[36] Lieb E H and Wu F Y 1968 *Phys. Rev. Lett.* **20** 1445
[37] Metzner W and Vollhardt D 1989 *Phys. Rev.* B **39** 4462
[38] Lindgren I and Morrison J 1982 *Atomic Many-Body Theory* (Berlin: Springer)
[39] Callaway J 1974 *Quantum Theory of the Solid State* (New York: Academic)
[40] Baeriswyl D 1987 *Nonlinearity in Condensed Matter* ed A R Bishop, D K Campbell, P Kumar and S E Trullinger (Berlin: Springer)
[41] Brazovskiĭ S A, Dzyaloshinskiĭ N E and Krichever I M 1982 *Sov. Phys.–JETP* **56** 212
[42] Jansen R W, Bertoncini R, Pinnick D A, Katz A I, Hanson R C, Sankey O F and O'Keeffe M 1987 *Phys. Rev.* B **35** 9830
[43] Hamada N, Sawada S and Oshiyama A 1992 *Phys. Rev. Lett.* **68** 1579
[44] Underhill A E, Clark R A, Marsden I, Allan M, Friend R H, Tajima H, Naito T, Tamura M., Kuroda H, Kobayashi A, Kobayashi H, Canadell E, Ravy S and Pouget J P 1991 *J. Phys. C: Solid State Phys.* **3** 933
[45] Tajima H, Naito T, Tamura M., Kobayashi A, Kuroda H, Kato R, Kobayashi H, Clark R A and Underhill A E 1991 *Solid State Commun.* **79** 337